Iodine Propellant Space Propulsion

IEPC-2013-311

Presented at the 33rd International Electric Propulsion Conference,
The George Washington University • Washington, D.C. • USA
October 6 – 10, 2013

James Szabo,[1] Mike Robin,[2] Surjeet Paintal,[3] Bruce Pote,[4] Vlad Hruby,[5] Chas Freeman[6]
Busek Co. Inc, Natick, MA, 01760, USA

Abstract: The near term potential for iodine propellant in Hall thrusters is explored. The merits of iodine with respect to other propellants are presented. Recent performance measurements are summarized, and new measurements taken with an eight kilowatt thruster are presented. Thruster discharge power exceeded 10 kW, and peak measured anode efficiency exceeded 65%. Spacecraft interactions issues are also addressed and relevant data taken with a one kilowatt thruster are presented. Plume data showed lower divergence with iodine than with xenon, and that a plume shield could effectively attenuate the far field plume. Material samples placed in the plume showed a strong reaction with iron, but little reaction with typical spacecraft materials. System level benefits including low storage pressure and extremely high density are also discussed. All results so far indicate iodine is a viable propellant for electric rockets, and for some missions is superior to xenon.

Nomenclature

$\vec{B}$	=	magnetic field
$\vec{E}$	=	electric field
$\vec{F}$	=	thrust
g_0	=	gravitational constant at Earth's surface, 9.81-m/s^2
I_b	=	beam current
I_d	=	discharge current
I_{sp}	=	specific impulse
$\vec{j}$	=	ion current density
$\dot{m}$	=	mass flow rate, subscripts a for anode
M	=	atomic or molecular mass
p	=	pressure
P	=	power
r	=	length of rotary arm on which Faraday probe is mounted (from rotation axis to probe tip)
T	=	temperature
V_d	=	discharge potential
α	=	fraction of incoming flux which condenses

[1] Chief Scientist for Hall Thrusters, jszabo@busek.com
[2] Research Engineer, AIAA Member
[3] Research Engineer, spaintal@busek.com
[4] Director, Hall Thrusters, bpote@busek.com
[5] President, vhruby@busek.com
[6] Laboratory Manager, cfreeman@busek.com

$\vec{\Gamma}$ = flux
$\vec{v}$ = velocity
μ = viscosity
θ = angle from beam centroid
η = efficiency

I. Introduction

THE Hall Effect Thruster (HET) is an efficient form of electric space propulsion that is typically used for orbit-raising and orbit maintenance. Today's flight HETs operate on the noble gas xenon (Xe) which is inert, heavy, and has a large ionization cross section. However, Xe is expensive and it must be stored in large, high pressure tanks. Consequently, a variety of alternatives have been proposed. This paper describes recent advances in Hall thruster systems fueled by the halogen iodine (I), with a focus on high power and spacecraft interactions testing. Iodine yields high specific impulse and efficiency, but stores at one thousandth the pressure and three times the density of Xe.

A. Hall Thrusters

A HET uses crossed electric and magnetic fields to generate and accelerate ions. Figure 1 represents the thruster geometries used in this research. The overall structure is defined by a magnetic circuit that produces a steady magnetic field $\vec{B}$ across an annular channel. The upstream portion of the channel is metallic and includes a gas distributor. This is the anode assembly. The outer anode passively shunts a portion of the magnetic field, creating a magnetic lens with a steep axial gradient in $\vec{B}$. The downstream portion of the channel is dielectric. A potential difference or discharge voltage V_d is applied between the anode assembly and a hollow cathode located outside the channel. The resulting electric field $\vec{E}$ is predominantly axial and is concentrated near the channel exit by interactions between the magnetic field and the plasma. In the channel, electrons are strongly magnetized and their transport is predominantly azimuthal due to the $\vec{E}\times\vec{B}$ Hall Effect. The extended electron path enables an efficient, impact driven ionization cascade. Ions are weakly magnetized and most are accelerated directly out of the channel, forming the ion beam. Specific impulse I_{sp} typically ranges from 1000-s to 3000-s, with higher values possible. Thrust $\vec{F}$ is generated by momentum exchange, making this an electric rocket.

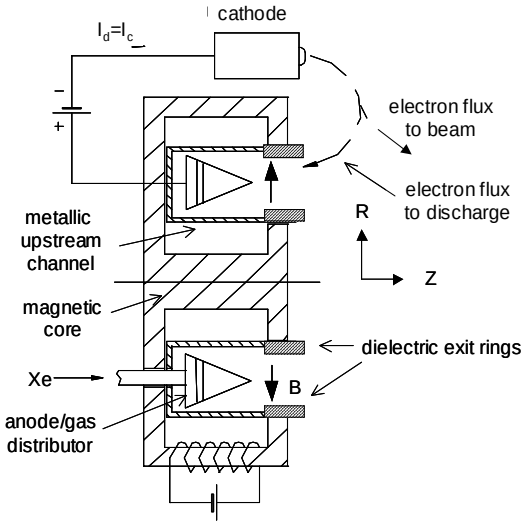

Figure 1. Nominal axisymmetric Hall Effect Thruster geometry.

The first American HET to fly in space was the nominal 200-W, xenon fueled Busek BHT-200.[1] This was also the first reported HET to be tested with iodine.[2] This paper reports iodine testing carried out with two higher power thrusters, the BHT-1000[3] and BHT-8000.[4]

B. Iodine Propellant Properties

The potential for iodine as a Hall thruster propellant was identified over a decade ago.[5,6] Table 1 compares key properties of iodine and xenon.[7,8,9,10] Atomic iodine (I) is lighter than Xe, but iodine stores and vaporizes as a diatomic molecule (I_2) for which the dissociation energy is 1.54-eV.[11] The ionization potential is lower for iodine, but the electron impact ionization cross section is larger.

Storage and handling properties for Xe and I_2 are very different. Xe must be stored in high pressure tanks or at cryogenic conditions. I_2 stores in the solid phase at approximately three times the density of Xe. The pressure of the I_2 reservoir may be 1000 times lower than the pressure in a Xe tank. I_2 vapor is generated by heating the solid to a modest temperature, e.g. 80 - 100 degrees C. The temperature of the I_2 flow path and gas distributor must be slightly higher to prevent the formation of condensed phases. However, the anode gas distributor does not have to be heated

during ordinary thruster operation. Because I_2 stores as a low pressure solid, the reservoir may be irregular in shape, conforming to available space. The propellant inside may even be used to shield electronics. A filled reservoir may in theory be stored for long periods of time in unregulated conditions on the shelf or in orbit.

In comparison with Xe, the vapor pressure of I_2 is extremely low, e.g. 1.2×10^{-6}-Torr at T =-75°C. This makes iodine much easier to pump inside a test facility. This, in turn, means lower background pressure and less test uncertainty. High power testing becomes feasible in facilities that would be completely inadequate for Xe.

Table 1. Properties of iodine and xenon.

Element	I	Xe
Atomic Mass	126.9	131.3
Ionization Properties (monatomic)		
First Ionization Potential (eV)	10.5	12.1
Peak Cross Section (10^{-16} cm^2)	6.0	4.8
Storage and Handling Properties		
Storage density (gm/cm^3) near room temp.	4.9	1.6*
Melting Point (°C)	113.7	-112
Boiling Point at 10 Pa (°C)	9	-181

*14 Mpa, 50 C (NIST Database)

I_2 is also comparatively low cost. I_2 at 99.99+ purity, demonstrated with the BHT-8000 (this paper), is several times cheaper than xenon. This is significant for high throughput missions.

The only significant disadvantage to iodine is its reactivity, though this may be addressed though materials selection. Safety precautions are not onerous.

C. Iodine Test History

Initial testing with the Busek BHT-200 showed that I_2 yields performance similar to Xe, with higher thrust to power F/P and/or efficiency η at some operating points.[2,12,13] Plume divergence was also lower with I_2. At nominal operating conditions, wetted probe measurements at the center of the plume found primarily I^+ with I_2^+ present at 3% by mole fraction.[2,12] Optical measurements were also taken, but no I_2 lines were observed.[14] In subsequent testing with an experimental variant of the BHT-200, the composition of the plume was analyzed in greater detail with wetted probes at multiple locations and operating conditions. Significant high energy I_2^+ fractions were found away from the beam centroid, sometimes exceeding 20% by mass.[15]

Most or all testing of the BHT-200 used a breadboard PPU that was a precursor to Busek's flight model, the BPU-600. This illustrates a key advantage that I_2 has with respect to many other alternative propellants: The PPU does not have to change.

Testing of the BHT-1000 focused on both performance and the plume. At most conditions, both η and F/P were higher with I_2 than with Xe.[16] Plume divergence was measured over multiple conditions and was consistently lower with I_2. The efficacy of a plume shield in attenuating the beam plasma was also explored; those results are presented here for the first time. In addition, material samples were exposed to the iodine plume; those results are also presented here for the first time.

Testing of the BHT-8000 is also reported here. The main focus was thruster performance. The thruster was successfully run at power levels exceeding 10-kW in the same facility used to test the BHT-200 and BHT-1000. This facility is inadequate for testing the BHT-8000 with Xe.

All of the above tests used xenon fueled BaO-W hollow cathodes. However, the overarching research program has also included I_2 fueled cathodes. As reported in Ref. 16, a high current LaB6 cathode was run on its own for over 1 hour with I_2 and for an additional half hour with a Xe thruster. More recently, CSU researchers developed a low temperature C12A7 electride hollow cathode that was tested for tens of hours with I_2.[17]

To feed all these systems, I_2 was sublimed from high purity crystals inside a thermally controlled reservoir located either inside or outside of the vacuum tank. The reservoir was connected to the anode by a heated flow line, but was electrically isolated by a ceramic break and/or section of non-conductive line. This allowed the feed system to be grounded.

II. Apparatus and Procedures

A. Hall Thrusters and Hollow Cathodes

The BHT-8000 is a single-stage HET that operates efficiently at power levels from 1-kW to 10-kW and discharge potentials up to 700-V.[4] The mean diameter of the discharge cavity is 170-mm. The hollow cathode is typically mounted along the geometrical thruster axis, a location shown to reduce beam divergence[18] and maximize

thrust efficiency. Electrical isolation of the anode from the propellant managements system is provided by a custom break that provides 2.5 kV or isolation with I_2.

The BHT-1000, used to investigate spacecraft interactions issues, operates efficiently at power levels from several hundred Watts to 2-kW and discharge potentials up to 1000-V. Here it was configured as a single stage thruster. It may also be configured as a two stage thruster.[3] The mean channel diameter is 68-cm, and the hollow cathode is mounted distal to the discharge. Electrical isolation of the anode is provided by a commercial-off-the-shelf (COTS) ceramic brake built by Insulator Seal Inc. (ISI) that provides 1.5 kV of isolation with I_2.

The hollow cathodes used with the thrusters were laboratory models flowing Xe. Both used porous tungsten hollow inserts impregnated with a low work function barium-calcium-aluminate mixture. The flow rate of Xe was typically 4 - 10% of the anode mass flow rate by mass.

B. Test Facilities

To accurately measure performance, the background pressure must be low, e.g. less than 5 x 10^{-5}-Torr. With I_2, this may be achieved in Busek's 1.8-m diameter T6 facility, which is equipped with both diffusion pumps and cryogenic pumps. With all cryogenic pumps operational, the rated Xe pumping speed is 90,000-l/s. Much I_2 testing was conducted with only the diffusion pump, which has theoretical pumping speed of ~17,000-l/s on air. Upstream of the diffusion pump is a large, liquid nitrogen cooled baffle which acts as a cryogenic pump for iodine. At liquid nitrogen temperatures (e.g. 77 K), the vapor pressure of I_2 (Figure 2) is effectively zero such that liquid nitrogen (LN_2) cooled surfaces act as sinks for non-energetic iodine.

T6 background pressure was measured with an INFICON Bayard-Alpert Pirani Combination Gauge, model BPG400, located at a flange on the side of the test facility downstream from the thruster. The gauge is calibrated for xenon but may be corrected for iodine. The estimated relative sensitivity of the gauge to I with respect to Xe is 1.19-1.34, and the estimated sensitivity to I_2 with respect to Xe is 2.41.[15]

The thrusters were powered by laboratory power supplies. The cathode was allowed to float with respect to facility ground. The inner and outer solenoid circuits were driven by separate direct current (DC) power supplies independent of the discharge. Figure 3 is a nominal power supply diagram for the BHT-8000.

BHT-8000 I_2 data were compared to Xe data taken previously in Busek's 2.4-m diameter, 200-kl/s T8 facility.[4] BHT-1000 Xe comparison data were taken in the T6 facility.

Research grade Xe for thrusters and cathodes was metered by Commercial Off-The-Shelf (COTS) mass flow controllers. High purity I_2 was provided by custom feed system components. The BHT-8000 was tested with 99.99+% pure I_2. The BHT-1000 was tested with 99.9985% pure I_2.

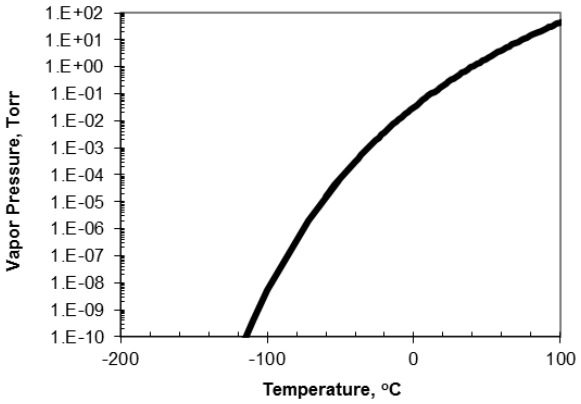

Figure 2. Iodine vapor pressure from Clausius–Clapeyron relation, Torr.

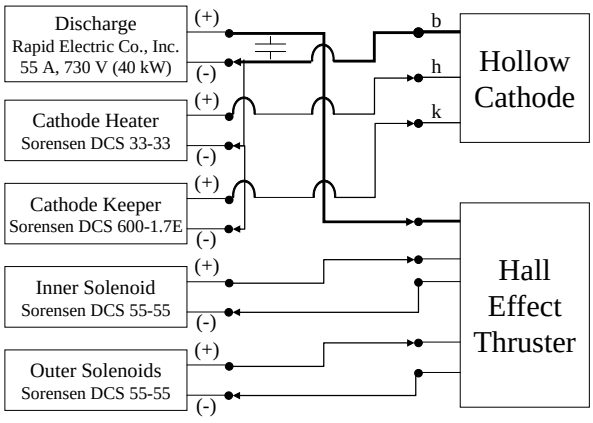

Figure 3. BHT-8000 nominal power supply diagram.

C. Iodine Propellant Management System

Busek's laboratory I_2 feed systems typically include a heated reservoir, thermocouples, pressure sensors, valves and feed lines. Coarse control of flow rate $\dot{m}$ is provided by adjusting the I_2 reservoir temperature. To decrease response time, fine control may be added in the form of a thermal throttle, as illustrated in Figure 4. This acts much like a proportional flow control valve (PFCV), a device demonstrated with I_2 in 2010.[2] Feedback may be provided by discharge current or by a mass flow sensor.

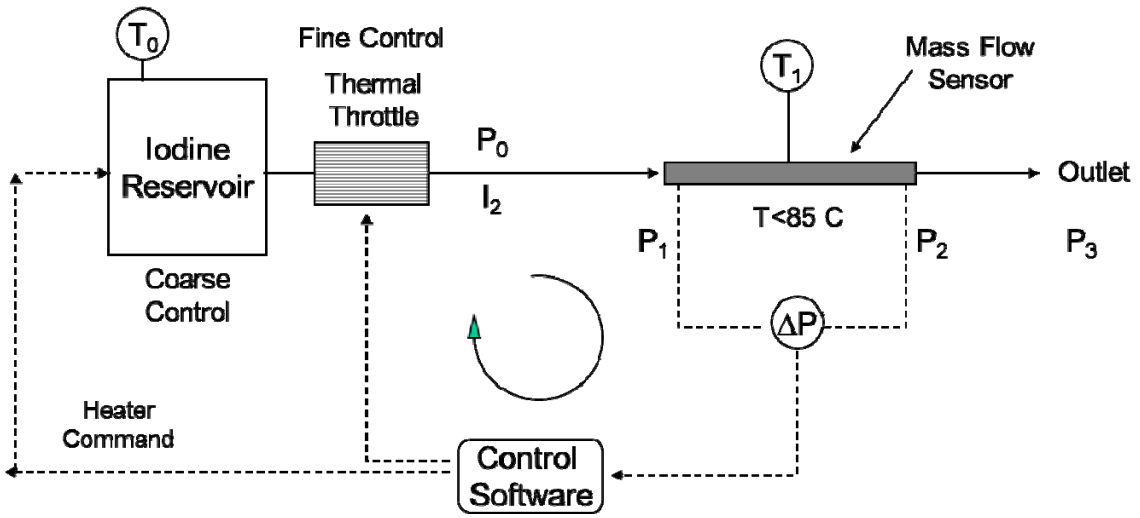

Figure 4. Feedback controlled I_2 feed system

For fully developed incompressible laminar flow in a horizontal pipe of radius R and length Δl, the pressure drop for a given mass flow rate is given by[2,19]

$$p_1^2 - p_2^2 = \dot{m}\frac{16\Delta l}{\pi R^4}\frac{\mu}{M}kT\gamma = \dot{m}C\,. \tag{1}$$

Here, μ is viscosity, M is molecular mass, T is gas temperature, and C is a constant. The factor γ is introduced to account for mismatches between the theoretical and actual geometry. The gas viscosity at T may be estimated from experimental data[20,21] using the Sutherland correction.[22] At typical feed system conditions, the ratio of viscosities is 0.60, with I_2 less viscous. A laminar flow sensor or section may be calibrated by measuring ($p_1^2 - p_2^2$) vs. $\dot{m}$. For multiple laminar flow segments in series with varying R, Δl and T, the relationship between upstream and downstream p^2 is still linear.

In the mass flow calibrations of Ref. 2, constant C was determined by monitoring pressure p_0 close to the reservoir, which was weighed before and after time interval Δt. Pressure at the thruster p_3 was estimated from isentropic flow theory. Figure 5 plots the Xe and I_2 calibration data of Ref. 2 against the theoretical form ($p_0^2 - p_3^2 = \dot{m}C$) changing only μ and M. The data fall on the theoretical curve, proving the validity of Equation 1.

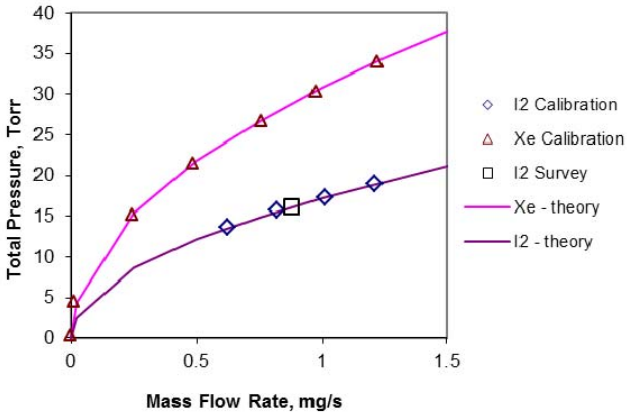

Figure 5. Calibrations of sensor pressure vs. flow rate for data of Ref. 2

For the BHT-8000 the flow rate was calibrated assuming that the pressure at the thruster is much less than the pressure at the reservoir, such that $p_0^2 \approx \dot{m}C'$. For the flow rates in question, the error in assuming $p_3^2 = 0$ is less than 1.4%. The flow rate calibration used for the BHT-1000 is not germane to the results reported here.

D. Performance Metrics

Thrust generated by the BHT-8000 was measured directly with an inverted pendulum, "Null" type thrust stand that is corrected for thermal drift.[23] Specific impulse was determined from thrust and mass flow rate by the equation

$$I_{sp} = F/\dot{m}g_0\,. \tag{2}$$

Here, g_0 is the force of gravity on the surface of Earth. Anode I_{sp} was calculated using only the anode flow rate. Efficiency was determined from thrust, mass flow rate, and input power P through the equation

$$\eta = F^2 / 2\dot{m}\, P \quad . \tag{3}$$

Here, P includes the power provided to the discharge ($P_d = V_d I_d$), electromagnets, and cathode. At the system level, PPU and feed system power losses would also be included. Efficiency calculated using only the anode propellant flow rate and discharge power is referred to as the anode efficiency. The ratio of thrust to power is related to efficiency and specific impulse by the equation

$$F / P = 2\eta / I_{sp} g_o \, . \tag{4}$$

The only way to increase F / P at constant I_{sp} is to increase efficiency.

E. Mission Assurance Testing and Metrics

A variety of tests were performed with the BHT-1000 to determine the shape of the iodine plume, whether it can be attenuated with a plume shield, and whether it will collect upon or react with the spacecraft. Figure 6 shows the test setup inside the chamber, which included a current probe, a plume shield, and material sample trays.

Ion current was measured with a nude Faraday probe[24] mounted on a rotating arm. The probe was positioned to sweep a $\Delta\theta$ =180° arc about the thruster exit, bisecting the plume. The length of the arm was approximately r =0.5-m, and the rotation axis was approximately 2-cm forward of the thruster exit plane.

To provide additional protection for sensitive spacecraft surfaces, the large angle plume may be attenuated with a plume shield.[25] The shape, size, and location of the plume shield are important. The shield tested with the BHT-1000 was a large sheet of stainless steel oriented parallel to the thrust axis. The shield was offset from the thruster centerline by 28-cm and extended 42-cm beyond the thruster exit plane.

To gauge the reactivity with iodine with thruster and spacecraft materials, samples were places in trays on both sides of the thruster such that one set was exposed to the raw plume and the other was shielded. Separate exposure tests were conducted with Xe and I_2. Before and after testing, the samples were weighed and photographed with a microscope. Sample materials included alumina, polyimide film, quartz, boron nitride, Hiperco 50A magnetic alloy, magnet iron, nickel, and stainless steel.

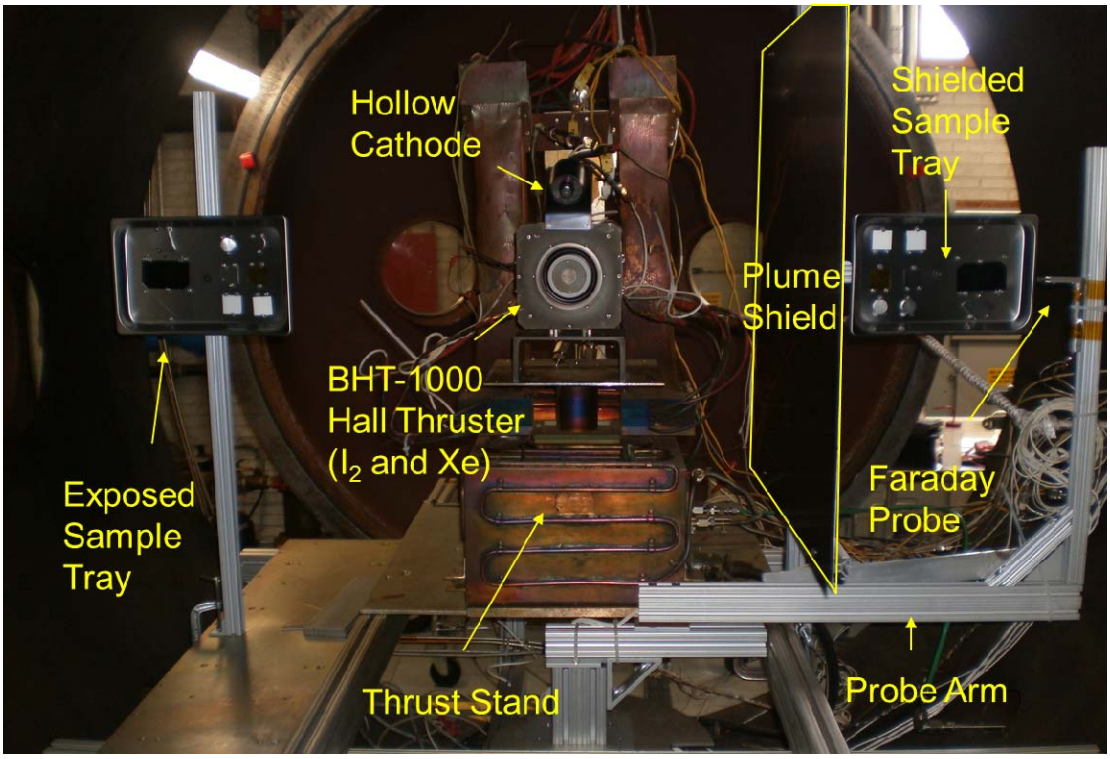

Figure 6. Chamber configuration for material exposure tests.

Beam divergence was calculated from ion current. One measure of plume divergence is the half angle θ_d which contains 90% of the integrated ion beam current. This may be determined by integrating beam current $j(\theta)$:

$$0.90 I_b = 2\pi r^2 \int_0^{\theta_d} j(\theta) \sin\theta d\theta \,. \tag{5}$$

Here, I_b is the integrated beam current, r is the sweep radius, and θ is the angle from the thruster centroid.

In the central portion of the plume, ion current decays exponentially with θ. At large angles, the plume is dominated by low energy ions presumably formed through charge exchange processes outside the thruster channel.[15] When calculating divergence, these charge exchange ions may be excluded from $j(\theta)$. One common method is to linearly extrapolate the logarithm of current, $\ln j(\theta)$, between $10 \le \theta \le 30$ degrees to $\pm 90°$.[26] If two or more sweeps are collected at different background pressures, then the "in space" plume current $j_0(\theta)$ may be determined for all angles by extrapolating either the current[27] or logarithm of current[28] to zero background pressure as a function of position.

III. High Power Test Results

A. Mass Flow Calibration

For performance testing, the flow system was calibrated by methods described in Section II.C.[2] Mass loss data were obtained while running the thruster at $\dot{m}_{I2}$ =8.0-11.2-mg/s. These data were correlated to pressure p_0 at the I_2 reservoir. A linear fit of p_0^2 vs. $\dot{m}$ was then generated yielding C =0.0177-mg/s/Torr^2. Figure 7 shows this fit along with an older calibration obtained via the mass flow sensor, which was inoperative during performance testing. The older data confirm that p_0^2 vs. $\dot{m}$ is linear, although the flow sensor slope was 3.4% higher. (The difference is within the estimated uncertainty). Significant scatter was associated with the calibration data and one data point was excluded, as discussed in Section III.C.

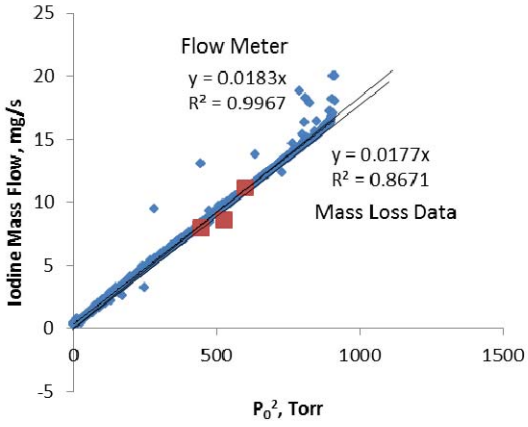

Figure 7. Mass flow calibration.

B. BHT-8000 Performance

Thrust was measured at power levels from P =1-kW to 9-kW. The peak demonstrated thruster power was 11.0-kW although thrust data were not taken at that power. Thrust data are plotted in Figure 8. Anode I_{sp} (Equation 2) is plotted in Figure 9, while anode η (Equation 3) is plotted in Figure 10. At V_d =500-V, anode I_{sp} can exceed 2500-s and anode η can exceed 66%. The uncertainty bars on the graphs show one estimated standard deviation σ.

In general, measured values for I_{sp}, η, and F/P (Equation 4) were similar to values measured previously with Xe.[4] A rigorous comparison is not made because Xe data were taken in a different facility with a different thrust stand at a different time. However, it is possible to make some point by point comparisons. For example, at V_d =405-V, P =7.0-kW, the measured performance with I_2 was F/P = 59-mN/kW +/- 1.2 mN/kW, I_{sp} =1940-s +/- 149-s, η = 56% +/- 5%. For the BHT-8000 flowing Xe at V_d =405-V, P =6.2 kW, the measured performance was F/P = 56-mN/kW +/- 1.2 mN/kW, I_{sp} =2123-s +/- 72-s, and η = 58% +/- 3%.

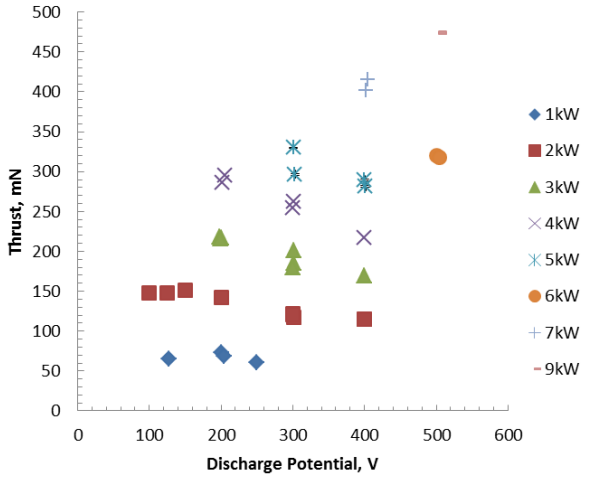

Figure 8. BHT-8000 thrust in mN with I_2.

Discharge current oscillations were measured with a current probe and a digital oscilloscope. (The capacitor bank shown in Figure 3 was not located in parallel with the discharge.) Figure 11 shows predator-prey[29] or breathing mode[30] oscillations found at V_d =500-V, $I_d \approx$ 15-A. The frequency is 20 to 25-kHz, which is the same range measured with Xe at V_d =600-V, $I_d \approx$ 15-A No attempt was made to minimize the oscillations by adjusting the solenoids. Previous BHT-200 testing showed I_2 and Xe oscillations to be similar in magnitude and frequency.[2]

Figure 12 shows the I_2 plume and discharge at V_d =300-V, $I_d \approx$ 15-A, The plume is visually similar in shape and hue to a Xe plume.

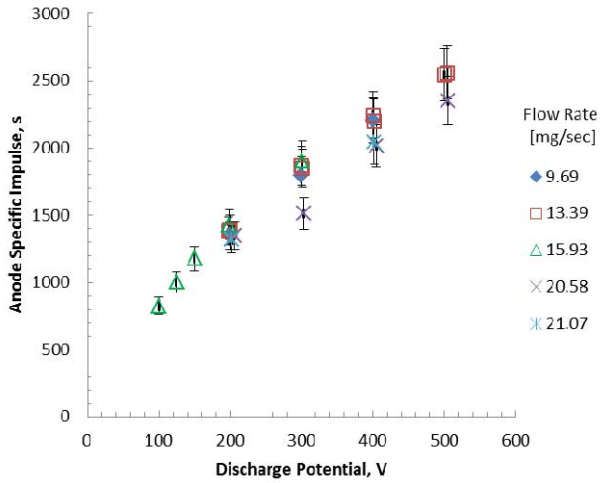

Figure 9. BHT-8000 anode I_{sp} in seconds with I_2.

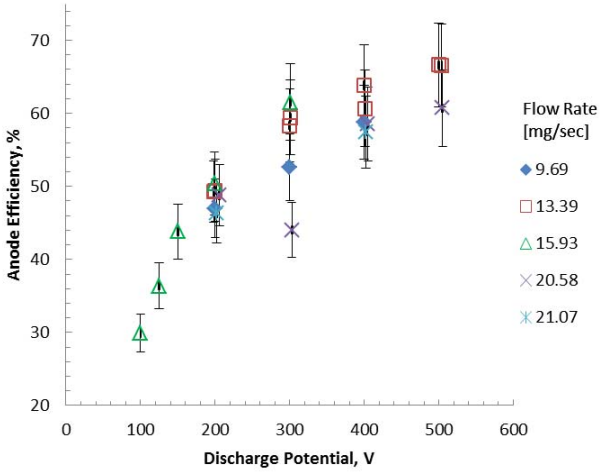

Figure 10. BHT-8000 anode efficiency with I_2.

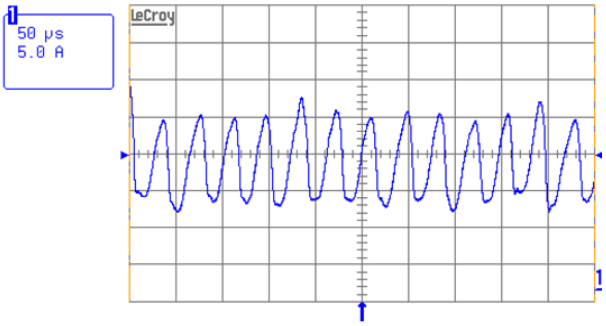

Figure 11. Discharge oscillations at 500-V, 15-A.

Figure 12. Iodine plume at 300-V, 15-A.

C. Uncertainty Estimation

The uncertainty associated with BHT-8000 performance measurements was estimated by standard methods.[31] Table 2 summarizes the calculation for P_d, F, $\dot{m}$, I_{sp}, and η.

The uncertainty in P_d is estimated to be 1.1%. The uncertainty in F is estimated to be 2.1%, which is not plotted because the error bars are comparable in size to the markers. Contributions were based upon prior testing of the BHT-8000 and other thrusters. The uncertainty in $\dot{m}$ is estimated to be 7.4%. Contributions include uncertainties in the calibration slope C, the pressure sensor reading, and propellant backflow. Uncertainties in I_{sp} and η are estimated to be 7.7% and 8.6%, respectively, both driven by uncertainty in $\dot{m}$.

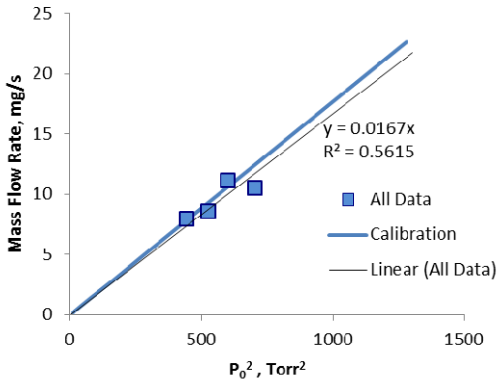

Figure 13. Mass flow calibration with all data.

Table 2. Uncertainties for performance.

Figure of Merit	Constituent	Normalized Variance (%)
Power	Voltage	0.5
	Current	1.0
	Standard Dev. (RMS)	**1.1**
Thrust	Slope of calibration curve	0.5
	Sample to sample variation	0.5
	Signal drift	2.0
	Standard Dev. (RMS)	**2.1**
Mass Flow Rate	Calibration Slope	7
	Sensor Output	0.3
	Backflow	1.1
	Standard Dev. (RMS)	**7.4**
Isp	**Standard Dev. (RMS)**	**7.7**
Efficiency	**Standard Dev. (RMS)**	**8.6**

The largest uncertainty is associated with the mass flow rate constant C, which was calculated with three mass calibration points plus the [0,0] point. An additional outlying data point was excluded. For the included $\dot{m}$ data, the normalized standard deviation is approximately 7% and the coefficient of determination R^2 is 0.87. Including the outlying point decreases R^2 to 0.56. Including the outlier also decreases the slope C by 5.6%, but the trend is away from the flow sensor calibration shown in Figure 7. Excluding the outlying data point increases the mass flow rate for a given value of p_0^2, which is more conservative. The full data set is shown in Figure 13 along with a linear fit to all data (C=0.0167-mg/s/Torr^2) that is not used. The calibration is in bold.

IV. Mission Assurance Test Results

A. Plume Divergence Measurements

The plume of the BHT-1000 was measured with I_2 and Xe at multiple operating points. The measured divergence was always less with I_2. At V_d =500-V, I_d =2-A, the difference was dramatic; the 90 degree divergence angle was 30° degrees with I_2 but over 50° with Xe. At V_d = 400-V, the difference was much smaller; thirty degrees enclosed 90% of the I_2 plume at I_d = 3.3-A, but only 86% of the Xe plume at I_d = 3.6-A. Table 3 summarizes the results for these and other conditions. Reported pressure is uncorrected for I or I_2. To calculate divergence in Table 3, tank effects were excluded from $j(\theta)$ by extending the exponential portion of $j(\theta)$ between 10° and 30° to ±90°, as discussed in Section II.F.

With iodine, the plume was measured at increments of both $\Delta\theta$ =1° and $\Delta\theta$ =5°. The results at 1° and 5° were close, showing the acceptability of the larger angular increment for rough comparisons.

At V_d =500-V, I_d =2-A, an extrapolation to "in-space" conditions with ln $j(\theta)$ was also performed The extrapolation was based upon two $\Delta\theta$ =1° degree iodine sweeps taken at different background pressures. The divergence of the in-space plume was then calculated using the same method as for the other plumes (i.e. by extrapolating the exponential portion between 10° and 30°). The resulting divergence was 32°. The in-space plumes calculated with both ln $j(\theta)$ and ln $j(\theta)$ are shown in Figure 14. The 10° and 30° extrapolation that yields 32° is also shown.

Table 3. Plume current summary.

Fuel	Discharge Potential [V]	Discharge Current [A]	Solenoid Current Inner [A]	Solenoid Current Outer [A]	Indicated Tank Pressure (Xe) [Torr]	Included Angle [deg]	Included Beam Fraction [%]	Sample Increment [deg]
Xe	504	2.02	4.0	4.0	2.4E-05	54	90	1
I2	506	2.02	6.9	5.1	3.2E-05	30	90	1
I2	506	2.02	6.9	6.1	3.2E-05	30	89	5
						35	94	5
I2	506	1.98	6.0	5.0	1.9E-05	29	90	1
Xe	403	3.29	4.0	6.0	5.8E-05	30	86	5
						35	92	5
I2	406	3.29	9.4	6.0	3.4E-05	30	90	5
I2	303	3.36	6.0	4.0	3.7E-05	35	89	5
						35	93	5

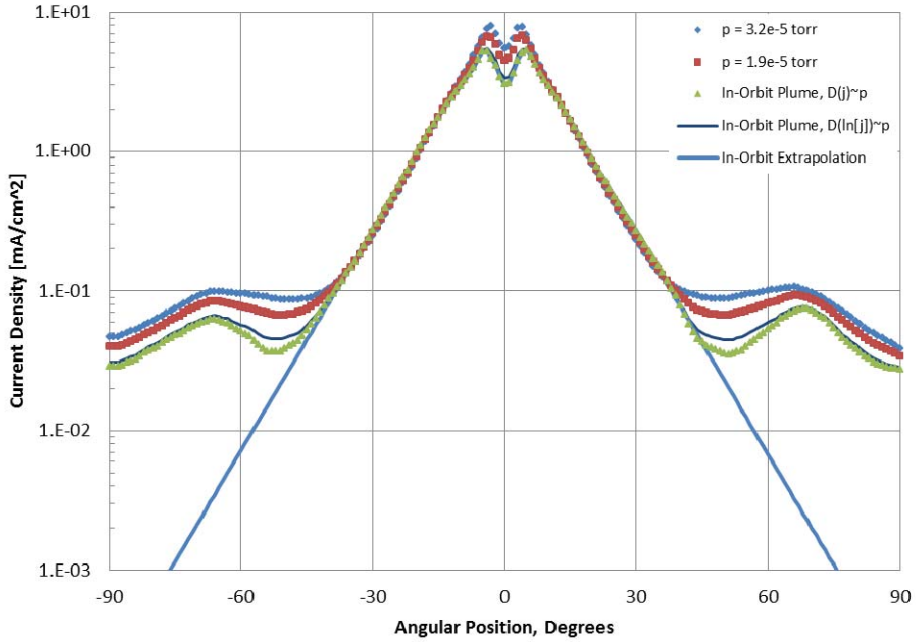

Figure 14. Plume current density at 500-V, 2.0-A showing I_2 in-space plumes and linear extrapolation used for divergence calculation.

B. Plume Shield Measurements

With the plume shield in place, BHT-1000 beam current with both I_2 and Xe was measured at three conditions: V_d =500-V, I_d =2-A; V_d =400-V, I_d =2.9-A; and V_d =300-V, I_d =2.9-A. The shield reduced the iodine far field current by approximately an order of magnitude. The shield was slightly less effective in shielding Xe, which could reflect a denser charge exchange plasma. Beam current with the shield in place is compared to beam current without the shield in Figure 15. In making this comparison, the measured current density was corrected by a factor of $(r/r_0)^2 = 2.25$ to account for an increased sweep radius r required for the probe to clear the shield. The sweeps are almost identical at large angles, but the plume current with the shield in place (larger r) is slightly lower in the center ($-15^o < \theta < 15^o$). This could reflect charge exchange losses, which increase with distance.

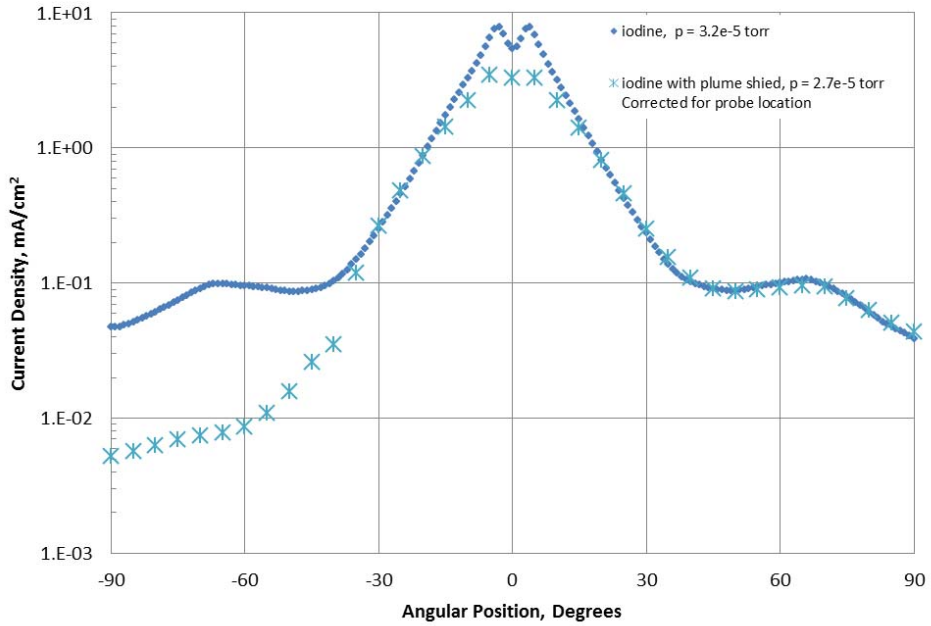

Figure 15. Plume current density (uncorrected) with and without plume shield, 500-V, 2-A, I_2.

C. Material Exposure Results

Iodine deposition on the material samples was extremely minor or non-existent. A slight reduction in mass was observed with magnet iron. The most significant visual reaction by far was also with magnet iron. Figure 16 shows iron and nickel samples exposed to Xe and I_2 at 100x magnification. The Fe sample appears to be heavily oxidized. The Ni sample appears essentially untouched except for some minor discoloration. Nickel coatings are one potential way to protect iron,

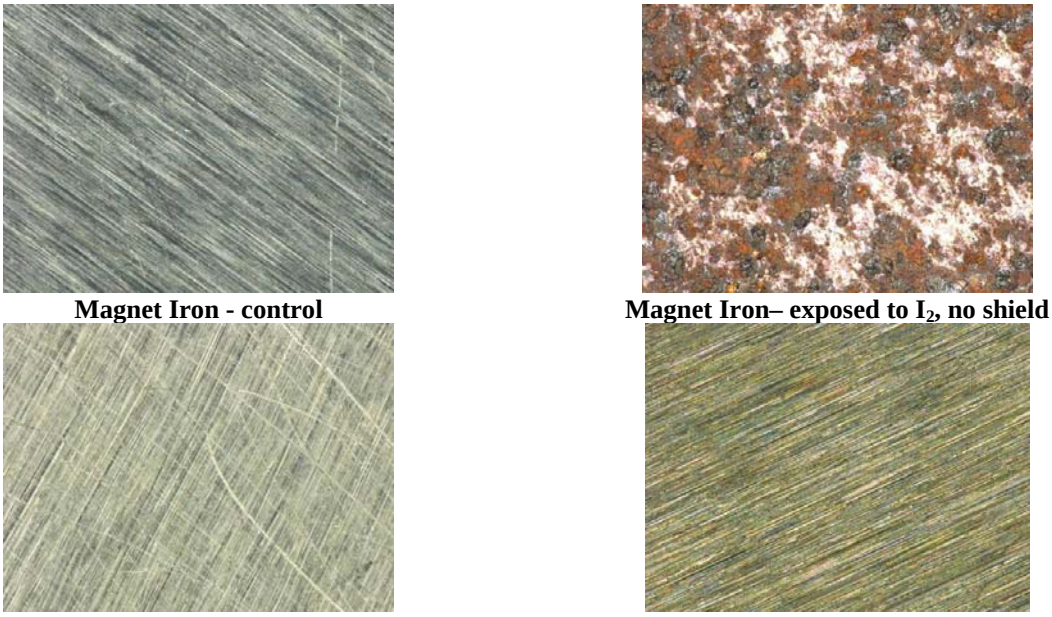

Magnet Iron - control | **Magnet Iron– exposed to I_2, no shield**

Nickel – control | **Nickel – exposed to I_2, no shield**

Figure 16. Magnet iron and nickel , Xe exposure (left) and I_2 exposure (right) at 100x magnification.

In considering these results, it should be noted that the environment inside the test facilities is not truly representative of in-space conditions. In space, the propellant travels away from the thruster and spacecraft, never to return. In a vacuum test facility, high energy ions are trapped and are likely to be reflected multiple times before they stick to cold surfaces. Thus, reaction rates are likely to be much lower on-orbit.

Conversely, it should also be noted that the sample exposure tests were very limited in duration. For most materials, no apparent reactions were observed after tens of hours. However, on a real mission, spacecraft surfaces would be exposed for thousands or tens of thousands of hours.

IV. Discussion

Performance data taken with the BHT-8000 and other thrusters indicate that I_2 is competitive with Xe. Plume testing paves the way toward actual missions.

A. Mission Applications

Potential applications for medium sized I_2 fueled thrusters include geostationary satellites, small orbital tugs, and deep space science missions. Examples destinations include high Earth orbits, the Moon, Mars, Venus, Near Earth Objects, and the asteroid belt. Small thrusters may be ideal for CubeSats or other small spacecraft where volume is at a premium. Large thrusters like the BHT-8000 can be clustered to 100-kW and above for large orbital tugs, planetary exploration, and asteroid retrieval.[32]

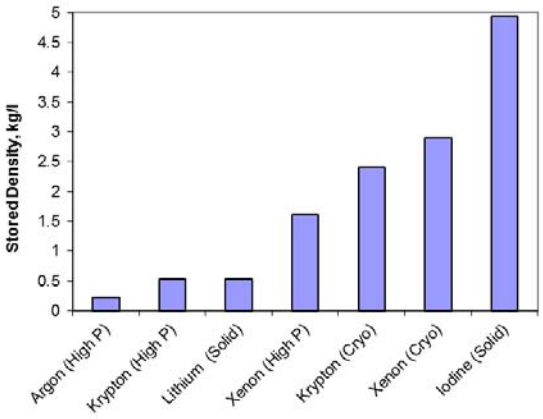

Figure 17. Stored density of electric rocket propellants in kg/l (high pressure at 14-MPa, 50°C).

When selecting the propellant for any mission, system level considerations like storage density, pressure, and temperature should be taken into account. At typical storage conditions (e.g. 14-MPa and 50°C) the stored density of Xe is 1.6-kg/l. At the same conditions, Kr stores at 0.5-kg/l. In stark contrast, solid I_2 has a density of 4.9-kg/l. The density of I_2 is compared to that of Xe, Kr and other electric rocket propellants in Figure 17.

For a high power, high throughput mission, the difference in stored propellant volume is enormous. For asteroid retrieval, Ref. 32 describes a system carrying 13 metric tons of Xe. This implies 8,100 liters of high pressure Xe or 4,600 liters of cryogenic Xe (2.9-kg/l). With I_2, the propellant volume could be as low as 2,600 liters. Furthermore, the I_2 could be stored at low pressure and tanks not in use could be unregulated.

B. Notional Flight System

In addition to the thruster and cathode, an iodine flight propulsion system would include at least four additional elements. These are the Power Processor Unit (PPU), Digital Control Interface Unit (DCIU), Iodine Feed System (IFS) and the propellant tank. The PPU distributes and regulates the power from the satellite power generation system to the thruster and support components. The DCIU provides an abstraction layer between high-level spacecraft commands and thruster low-level actuation. The IFS provides isolation, metering and active flow control of the propellant. The propellant tank provides iodine storage. Figure 18 shows a notional panel mounted I_2 system for a 100 to 200-kg spacecraft including all these components and more. The PPU, heater control

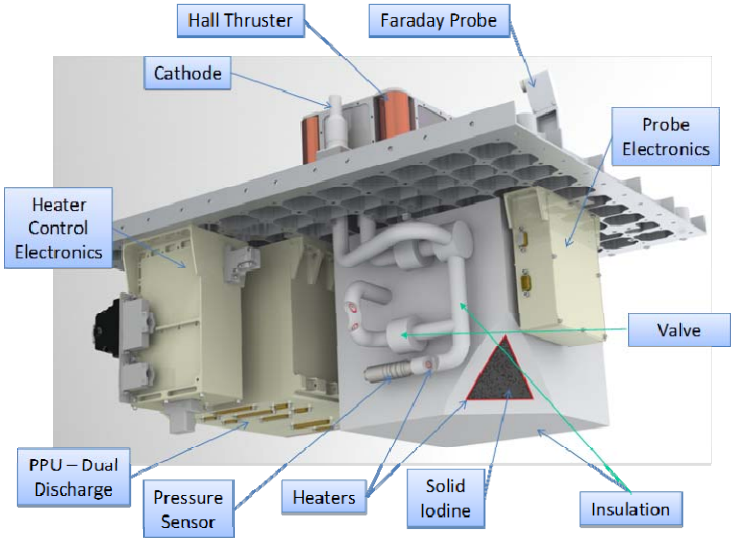

Figure 18. Notional layout of iodine HET flight system for ESPA class spacecraft.

electronics, plasma probe, and probe electronics all have flight heritage. The propellant tank is sized to hold 40-kg of I_2. The system would notionally include a separate heater control electronics module for the IFS and propellant reservoir. It would also include a wetted plasma probe or probes for on-orbit plume characterization.

The flight thruster may be oriented to minimize plume impingement upon spacecraft surfaces. Fortunately, I_2 yields lower beam divergence than Xe. This result has been measured consistently with all thrusters tested, although background pressure could be a significant factor. The flight system may also include a plume shield to provide extra protection to sensitive spacecraft surfaces. Ion current measurements taken with the BHT-1000 prove that a shield may attenuate the plasma. Attenuation should be even greater in space, where the charge exchange plasma is more tenuous and the background does not include atmospheric trace gases and primary beam ions that have not yet shed enough energy to be collected at cold surfaces. Potential material interactions would be addressed though coatings and materials selection.

C. Iodine Deposition and Removal

To avoid bulk accumulation of I_2 on surfaces, the removal rate must exceed the arrival rate. The flux away from a surface may be estimated from the I_2 vapor pressure.[33,34]

$$\Gamma_{out} = \alpha \frac{(p_v - p_\infty)}{\sqrt{2\pi MkT}}. \tag{6}$$

In this equation, p_v is the vapor pressure of the solid at temperature T, p_∞ is the partial or background pressure, M is the molecular mass, k is the Boltzmann constant and α is a constant expressing the fraction of incident ions or molecules which condenses. The conservative limit is $\alpha = 1$. Γ_{out} is zero when the background pressure is equal to the vapor pressure. However, although p_∞ is close to zero in space, there may still be a charge exchange plasma with an arrival rate given by

$$\Gamma_{in} = \frac{j}{eZ}. \tag{7}$$

If the arriving substance is monatomic and the evaporating substance is diatomic, then to remain clean, $\Gamma_{out} > 0.5\ \Gamma_{in}$, such that

$$2eZ \frac{p_v}{\sqrt{2\pi MkT}} > j. \tag{8}$$

Figure 19 plots this relation. The curve represents the threshold current density for a surface at temperature T above which mass starts collecting. Below this threshold, accumulation may be only a few monolayers or less.[35] BHT-1000 measurements can be used to estimate j in the vicinity of a thruster and, in turn, the critical temperature. In the large angle plume at V_d =500-V, I_d =2-A, the in-space plume current density (Figure 14) was 0.05-mA/cm^2. For this threshold, Figure 19 says T must be greater than -75°C. Most spacecraft surfaces will be far warmer. Therefore, I_2 will not accumulate.

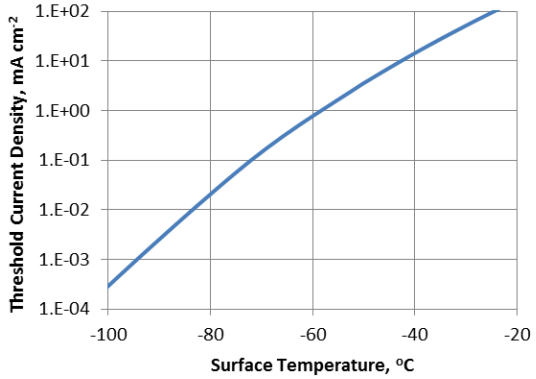

Figure 19. Threshold current density for bulk accumulation in mA/cm^2.

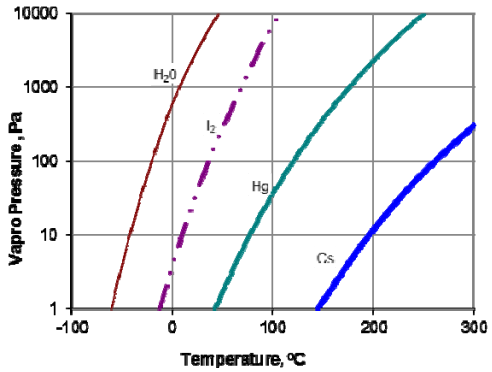

Figure 20. The vapor pressure of I_2 and other electric rocket propellants in Pascals[8].

At typical spacecraft surface temperatures, the vapor pressure of I_2 in Pa is two decades higher than that of Hg and four decades higher than that of Cs, both of which have been tested in space with ion engines. The vapor pressures are plotted in Figure 20. The comparison with Hg is especially significant because Hg ion engines on the SERT II spacecraft were successfully fired on-orbit for 4000 hours.[36] Most spacecraft surfaces were too warm to permit Hg condensation and showed no evidence of condensate.[36] The exception to this was a cold collector experiment intended to measure potential Hg back-contamination, but the experiment was overwhelmed by Mo from the grids. The solar arrays were far too warm for condensation; their temperature was consistently at or above 310 K.[36] SERT II proved that condensable propellants are a viable option for space propulsion.

V. Conclusions

A variety of Hall thrusters have been tested with I_2. Prior performance data taken with low and medium power thrusters showed that I_2 is competitive with Xe. New data taken with the BHT-8000 extend the result to power levels of 10-kW per thruster.

Mission Assurance testing with I_2 has focused on plume measurements and analysis. Tests reported here used the medium power BHT-1000. The beam was found to be less divergent with I_2, and a plume shield was shown to be effective means for attenuating the beam current at large angles. Analysis indicates that deposition upon the spacecraft should be minor or non-existent. Spacecraft relevant material samples were exposed to the plume, and the only serious reaction was found with magnet iron.

Test results so far indicate iodine is a viable propellant for electric rockets. For some missions iodine will be superior to xenon. System level advantages include dramatic reductions in system size, mass, and cost. A near term technology demonstration could be based, in large part, upon existing hardware.

Acknowledgments

BHT-1000 plume measurements were supported by the United Launch Alliance. BHT-8000 iodine testing was supported by NASA.

References

[1]Monheiser, J., Hruby, V., Freeman, C., Connolly, W., and Pote, B., "Low-Power Hall Thruster System," in *Micropropulsion for Small Spacecraft*, ed. M. Micci and A. Ketsdever, *Progress in Astronautics and Aeronautics*, V. 187, 2000.

[2]Szabo, J., Pote, B., Paintal, S., Robin, M., Hillier, A., Branam, R., Huffman, R., "Performance Evaluation of an Iodine Vapor Hall Thruster", *AIAA Journal of Propulsion and Power*, Vol. 28, No. 4, July/August 2012, pp. 848-857. doi: 10.2514/1.B34291

[3]Pote, B., and Tedrake, R., "Performance of a High Specific Impulse Hall Thruster," *Proceedings of the 27th International Electric Propulsion Conference*, Electric Rocket Propulsion Society, IEPC-01-35, October 2001.

[4]Szabo, J., Pote, B., Byrne, L, Paintal, S., Hruby, V., Tedrake, R., Kolencik, G., Freeman, C. "Eight Kilowatt Hall Thruster System Characterization," *Proceedings of the 33rd International Electric Propulsion Conference*, Electric Rocket Propulsion Society, IEPC Paper 2013-317, October 2013.

[5]Tverdokhlebov, O. S. and Semenkin, A. V., "Iodine Propellant for Electric Propulsion – To Be Or Not To Be," *37th AIAA/ASME/SAE/ASEE Joint Propulsion Conference*, AIAA-2001-3350, 2001.

[6]Dressler, R., Chiu, Y.-H., Levandier, D., "Propellant Alternatives for Ion and Hall Effect Thrusters," *28th Aerospace Sciences Meeting & Exhibit*, AIAA- 2000-0602, Reno, NV, 2000.

[7]Joshipura, K. N., Limbachiya, C. G, "Theoretical total ionization cross-sections for electron impact on atomic and molecular halogens," *International Journal of Mass Spectrometry*, 216 (2002), pp. 239-247.

[8]*CRC Handbook of Chemistry and Physics*, 83rd Edition, CRC Press LLC, 2002.

[9]Syage, J., "Electron-impact cross sections for multiple ionization of Kr and Xe," *Phys. Rev. A*, 46, 9, 1992, pp. 5666-5679.

[10]Hayes, T., Wetzel, R., Freund, R., "Absolute electron-impact-ionization cross-section measurements of the halogen atoms," *Physical Review A*, 35, 2, January 15, 1987, pp, 578-584.

[11]Frost, D., and McDowell, C., "The Ionization and Dissociation of some Halogen Molecules by Electron Impact," *Canadian Journal of Chemistry*, 1960, 38(3): 407-420, 10.1139/v60-057

[12]Hillier, A., Branam, R., Huffman, R., Szabo, J., and Paintal, S., "High Thrust Density Propellants in Hall Thrusters," *49th AIAA Aerospace Sciences Meeting including the New Horizons Forum and Aerospace Exposition*, AIAA- 2011-524, January 2011

[13]Hillier, A., "Revolutioning Space Propulsion Through the Characterization of Iodine as Fuel for Hall-Effect Thrusters," M.S. Thesis, Air Force Institute of Technology, Wright-Patterson Air Force Base, Ohio, 2011.

[14]Chiu, Y., Prince, B., "Optical Emission Spectra of the Iodine Hall Effect Thruster," *48th AIAA/ASME/SAE/ASEE Joint Propulsion Conference*, AIAA-2012-3872, July 2012.

[15]Szabo, J., Robin, "Iodine Plasma Species Measurements in a Hall Effect Thruster Plume," *49th AIAA/ASME/SAE/ASEE Joint Propulsion Conference*, AIAA-2013-4114, July 2013.

[16] Szabo, J., Robin, M., Paintal, Pote, B., S., Hruby, V., "High Density Hall Thruster Propellant Investigations," *48th AIAA/ASME/SAE/ASEE Joint Propulsion Conference*, AIAA-2012-3853, July 2012.

[17] Rand, L, Williams, J., "Instant Start Electride Hollow Cathode", *Proceedings of the 33rd International Electric Propulsion Conference*, Electric Rocket Propulsion Society, IEPC-2013-305, October 2013.

[18]Hofer, R., Johnson, L., Goebel, D., Wirz, R.., "Effects of Internally Mounted Cathodes on Hall Thruster Plume Properties," *IEEE Transactions on Plasma Science*, Vol. 36, No. 5, October 2008.

[19]Fox, R., and McDonald, A., *Introduction to Fluid Mechanics, 3rd Edition*, John Wiley & Sons, New York, 1985, p. 360.

[20]Rankine, O., "On the Viscosity of the Vapour of Iodine," *Roy. So., Proc. 91*. pp. 201-208, March 1, 1915.

[21]Kestin, J., Ro, S., and Wakeham, W., "Viscosity of the Noble Gases in the Temperature Range 25-700^{o}C," *Journal of Chemical Physics*, 56, 8, 15 April 1972, pp. 4119-4124.

[22]Sutherland, W., "The Viscosity of Gases and Molecular Force," *Philosophical Magazine Series*, 5, 36:223, 507-531.

[23]Haag, T., *Rev. Sci. Instrum*. 62, 1186, 1991.

[24]Azziz, Y., "Experimental and Theoretical Characterization of a Hall Thruster Plume," Ph.D. Dissertation, Department of Aeronautics and Astronautics, Massachusetts Institute of Technology, Cambridge, MA, 2007.

[25]Pollard, J., and Diamant, K., "Hall Thruster Plume Shield Wake Structure," *39th AIAA/ASME/SAE/ASEE Joint Propulsion Conference*, AIAA-2003-5018, July 2003.

[26]McVey, J., Britt , E., Engelman, S., Gulczinski, F., Beiting, E. and Pollard, J., "Characteristics of the T-220HT Hall-Effect Thruster," *39th Joint Propulsion Conference*, AIAA-2003-5158, July 2003.

[27]Azziz, Y., Martinez-Sanchez, M., Szabo, J., "Determination of In-Orbit Plume Characteristics from Laboratory Measurements," *42nd AIAA Joint Propulsion Conference*, AIAA-2006-4484, July 2006.

[28]De Grys, K., Tilley, D., Aadland, R., "BPT Hall Thruster Plume Characteristics," *35th Joint Propulsion Conference*, AIAA-99-2283, June 1999.

[29]Fife, M. Martinez-Sanchez, M., Szabo, J., "A Numerical Study of Low-Frequency Discharge Oscillations in Hall Thrusters," *33rd AIAA/ASME/ASE/ASEE Joint Propulsion Conference*, AIAA Paper 97-3052, July 97.

[30]Boeuf, J. P.; Garrigues, L. , *Journal of Applied Physics* , vol.84, no.7, pp.3541-3554, Oct 1998.

[31]Wilson, E., *An Introduction to Scientific Research*, New York: McGraw Hill, 1952, pp. 272-274.

[32]Brophy, J., et al., "Asteroid Retrieval Feasibility Study," Keck Institute for Space Studies, JPL, April 2012.

[33]Miyamoto, S., "A Theory on the Rate of Sublimation," *Trans. Faraday Soc.*, 1933, 29, 794-797, DOI: 10.1039/TF9332900794

[34]Staggs, J., Gula, W., Kerslake, W., "The Distribution of Neutral Atoms and Charge-Exchange Ions Downstream of an Ion Thruster," *AIAA 5th Aerospace Sciences Meeting*, AIAA-67-82, January 1967

[35]Hall, D., Newnam, B., Womack, J. "Electrostatic Rocket Exhaust Effects on Solar-Electric Spacecraft Subsystems," *J. Spacecraft*, Vol. 7, No. 3, March 1970, pp. 305-312.

[36]Kerslake, W., and Ignaczak, L., "Development and Flight History of SERT II Spacecraft,", *28th AIAA/SAE/ASME/ASEE Joint Propulsion Conference and Exhibit*, AIAA-92-3516, July 1992.